Available online at www.sciencedirect.com

ScienceDirect

Energy Procedia 53 (2014) 70 – 85

Energy Procedia

EERA DeepWind'2014, 11th Deep Sea Offshore Wind R&D Conference

The Impact of Active Power Losses on the Wind Energy Exploitation of the North Sea

Hossein Farahmand[a]*, Leif Warland[a], Daniel Huertas-Hernando[a]

[a] *SINTEF Energy Research, Sem Sælands vei 11,P.O.Box 4761 Sluppen,7465 Trondheim, Norway*

Abstract

Transmission active power losses can influence the distribution of power flows in the transmission grid which consequently alter the generation dispatch and scheduling through the power system. This can especially affect the exploitation of large scale renewable energy sources (RES) since they are normally installed far away from load centres. RES technologies are expected to cover a large portion of the future energy mix in the continental European power system and grid bottlenecks are a critical factor for successful integration of RES technologies in Europe. In this respect, transmission losses can significantly affect the potential grid bottlenecks and the exploitation of the expected energy produced by RES.

In this paper a comparison analysis is carried out on approaches to include active power losses in a DC optimal power flow. The initial idea is to apply a method to the existing flow-based market model Power System Simulation Tool (PSST), a tool for studying the effect of high penetration of wind power and consequent grid expansion in the European power system. Implementation of losses in large scale power systems significantly increases the computational burden. A solution to reduce computational time is to calculate reasonably good approximations of the active power losses. This paper proposes an approach to include transmission active power losses that can be implemented in large scale power system in reasonable computational time.

Selection and peer-review under responsibility of SINTEF Energi AS

Keywords: Transmission active power losses; DC-optimal power flow; Linearized loss approximation; Offshore wind production; power generation dispatch

Nomenclature

NG	number of generators
NB	number of busses

* Corresponding author. Tel.: +47-930-06538; fax: +47-735-97250.
E-mail address: Hossein.Farahmand@sintef.no

Selection and peer-review under responsibility of SINTEF Energi AS
doi:10.1016/j.egypro.2014.07.216

C_i	generation cost at Bus i (EUR/MWh)
G_i	generation dispatch at Bus i (MWh)
D_i	demand at Bus i (MWh)
θ_i, θ_j	voltage angles at Buses i and j, respectively (radian)
D_i	demand at Bus i (MWh)
B_{ij}	susceptance of transmission line ij (Ω^{-1})
$\underline{G_i}, \overline{G_i}$	maximum and minimum generation output at Bus i (MW)
$\overline{P_{Lij}}$	active power loss on transmission line ij (MWh)
I_{Lij}	current on transmission line ij (A)
r_{ij}	resistance of transmission line ij (Ω)
x_{ij}	reactance of transmission line ij (Ω)

1. Introduction

The increased integration of wind power, both onshore and offshore, and the demand for improved power system operation give rise to a growing need for transnational power exchanges [1]. In this paper, a comparison study has been carried out between different methodologies which calculate active power losses in power system analysis. Focus is the impact of power losses on the exploitation of the wind energy potential in the North Sea [2].

The inclusion of losses effectively changes both the total generation cost and the optimal generation dispatch as compared to the lossless situation. The active power losses can influence the distribution of power flows along transmission lines and energy mix throughout power systems. Therefore, the losses can especially affect the exploitation of potential energy produced by large scale RES, since they are usually located far away from load centers. This is the main motivation for including losses in this study. Ideally, AC optimal power flow (OPF) should be used to calculate power flow and active power losses in the transmission system. However, AC optimal power flow is nonlinear optimization problem which requires extensive computational effort when solving large scale power systems. A solution to reduce computational burden is to calculate reasonably good approximation of the active power losses [3]. Thus, trade-off between the computational time and the accuracy of the results is necessary.

The AC power flow equations can be approximated by set of linear DC power flow. DC power flow represents a reasonably accurate approximation of AC power flow [4]. DC power flow equations retain the convexity of optimization problems and can be embedded in optimal power flow calculation. The major advantage of DC optimal power flow models is the possibility of obtaining solutions fast and without using iterative processes. These features are of great value when such models are applied to large scale systems where the OPF problem needs to be solved under various operating conditions and several times. However, DC power flow models do not account for active power losses. The challenge arises when: *i)* trying to keep computational effort within reasonable time; *ii)* accurately model active power losses. This paper presents a methodology to include active power losses in DC optimal power flow calculation that can be implemented in large scale power system with reasonable computational time.

This paper is organized as follows. Section 2 introduces the DC-OPF problem. Approaches to include transmission power losses into DC-OPF problems are outlined in Section 3. The simulation toolbox to implement the approaches proposed in the previous section presented in Section 4. Subsequently, the approaches are tested on benchmark IEEE test system and their performance are assessed and discussed in Section 5. Moreover, the approaches are applied on Northern European power system, as example of a relevant large scale system where impacts of transmission losses are discussed in relation with offshore wind and interconnection utilization. Section 6 concludes the paper.

2. DC OPF model

Fig. 1 shows a two-bus system, and equivalent circuit of a transmission line, between bus i and bus j with a lumped parameter represented by the series impedance Z_{ij}. The major approximation in a DC power flow is to neglect reactive power and transmission line resistance, as well as the assumption of a flat voltage profile at all

nodes (all voltage magnitudes are equal to 1.0 per unit) which is particularly the case for light load condition. Additionally, the voltage angle difference ($\Delta\theta_{ij} = \theta_i - \theta_j$) is assumed to be small [5].

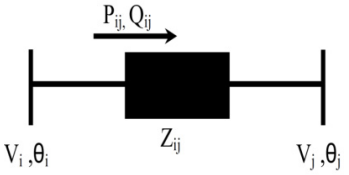

Fig. 1. Branch impedance ignoring shunt elements

Fig. 2 illustrates the simplified transmission line model between buses *i* and *j* in DC power flow calculation.

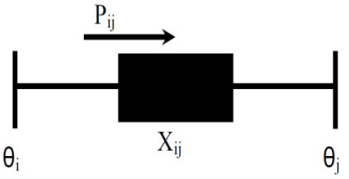

Fig. 2. Simplified DC power flow representation of transmission lines

Based on the above assumption, a linear DC power flow can be used in optimization problems instead of non-linear AC power flow equations. A DC optimal power flow is described in general form as in Eqs. (1) [5].

$$
\begin{aligned}
&Min \sum_{i=1}^{NG} \left(c_i \times G_i \right) \\
&\text{s.t.} \\
&\sum_{j=1}^{NB} B_{ij} \left(\theta_i - \theta_j \right) = P_i - D_i \quad i = 1 \ldots NB \\
&\underline{P}_{ij} \le B_{ij} \left(\theta_i - \theta_j \right) \le \bar{P}_{ij} \quad i, j = 1 \ldots NB \\
&\underline{G}_i \le G_i \le \bar{G}_i \quad i = 1 \ldots NG
\end{aligned}
\tag{1}
$$

The cost elements c_i are typically given by the marginal cost of production units. In the optimization problem the voltage angles, *i.e.* θ are introduced as part of the state variables defining the power flow through branches. In general, the Eqs. (1) can be written as linear programming (LP) model as shown below in Eqs. (2).

$$
\begin{aligned}
&\text{Min } F\left(\underline{c}^t \underline{x} \right) \\
&\text{s.t.} \\
&\underline{B}_{low} \le \underline{A}\underline{x} \le \underline{B} \\
&\underline{x}_{lb} \le \underline{x} \le \underline{x}_{ub}
\end{aligned}
\tag{2}
$$

The DC Power flow is the part of the equality constraints where $\underline{B}_{low}$ and $\underline{B}$ are identical. The branch flow limits and generation installed capacity limits are given by the inequality constraints.

3. Active power losses

The active loss dissipated in a branch, shown in Fig. 1, is proportional to the square of the current flowing through the branch, as given by Eq. (3) [5].

$$P_{Lij} = r_{ij} \cdot I_{ij}^2 \approx r_{ij} \frac{\Delta\theta^2}{x_{ij}^2} = r_{ij} \frac{\left(\theta_i - \theta_j\right)^2}{x_{ij}^2} \quad (3)$$

In this paper we aim to attach this quadratic curve to the LP optimization model. Two approaches can then be followed to handle losses within an LP optimization process: *i)* either account for the losses by including constant loss iteratively to the optimization problem [6, 7] or *ii)* include the losses as a part of the optimization by taking into account the linearized approximation of losses [8-10].

Another approach found in literature is to incorporate piecewise linearization of transmission losses by discretizing of the flow variables where each flow variable segment is assigned to a loss coefficient [11, 12]. The main drawback of this approach is the large number of variables which needs to be added to the optimization problem in the case of large scale power system [3].

3.1. Including constant power losses by iteration

Fig. 3 depicts the algorithm to apply the transmission losses to the optimization problem. Basically, the losses are calculated out of the optimization routine and are not integrated into optimal generation scheduling problem. As shown in Fig. 3, the results from DC-OPF are considered as an initial result to estimate losses. The allocated loss on each transmission line is updated using Eq. (3). Half of the losses are added at each end of the transmission line as shown in Fig. 4. When the differences in the power flow between two optimal power flow solutions are below a certain threshold, the solution has been found. This process is usually fast and converges in a few iterations. However, it is not necessarily yield the global optimal solution to the original problem. Generation and demand are not necessarily dispatched in an optimal way to reduce power losses since the optimization problem is updated exclusively with new information on the updated value of losses and no feedback from the active power losses calculation is considered in the optimization routine.

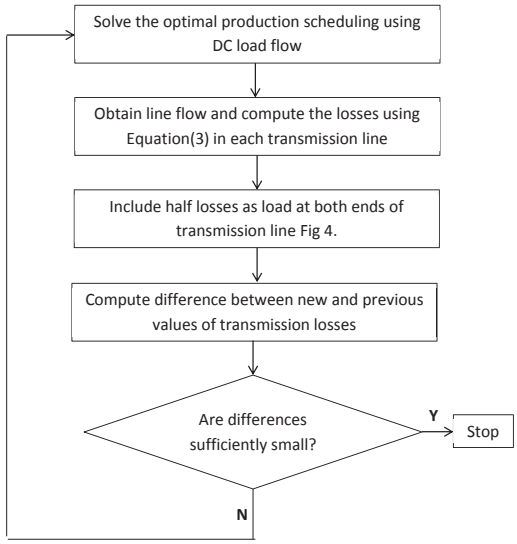

Fig. 3. Including constant losses using interactive process in DCOPF

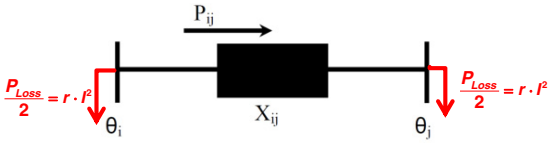

Fig. 4. Loss represented as loads at both ends of transmission line

In order to overcome these drawbacks in the transmission loss calculation, we propose the next approach (*Section 3.2*) which is based on the linear approximation of the losses.

3.2. Linearized approximation of transmission power losses

This approach is based on linearized approximation of transmission power losses around a power system operating point using Taylor expansion, as shown in Fig. 5. The red curve shows the quadratic loss, as given by Eq. (3), and the green curve shows the linearized loss, as given by Eq. (4). Here $a=\partial P_{Lij}/\partial\theta$ and b is the estimated offset for transmission losses representation. The optimization problem will, this way, receive a feedback on either the increase or decrease in the objective function "$F(\underline{c}^t \underline{x})$" due to changes in power flow and branch loss dissipation.

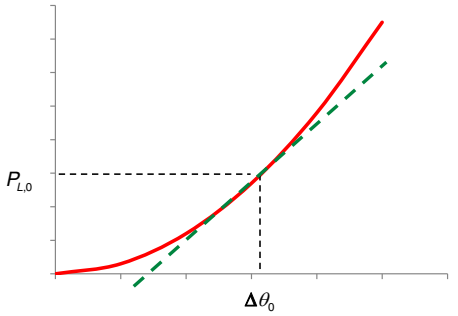

Fig. 5. Linearized transmission losses

$$P_{Lij} \approx b + a\Delta\theta = -r_{ij}\frac{\Delta\theta_0^2}{x_{ij}^2} + 2r_{ij}\frac{\Delta\theta_0}{x_{ij}^2}\Delta\theta \tag{4}$$

The calculated power, as given in Eq. (3), can flow in both directions depending on the sign of $\Delta\theta$. However, the contribution to power losses is proportion with the square of the power. Whereas this is not the case with the linearized losses shown in Eq. (4), since the power losses can be negative depending on the sign and size of $\Delta\theta$. This is not a physical situation. To handle this issue within the optimization problem, two state variables x_1 and x_2 are added, both positive $x_{1,2} > 0$, where its difference represents the flow on the branch. This introduces an additional equality constraint, expressed by Eq. (5). Eq. (5) connects now the "flow" description with the voltage angles and the two new state variables for transmission loss description.

$$\theta_i - \theta_j - (x_1 - x_2) = 0 \tag{5}$$

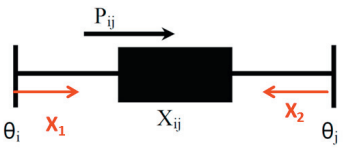

Fig. 6. Loss represented as linearized transmission losses around the power system operating point

Fig. 6 shows the transmission loss representation using linearized losses where both x_1 and x_2 are assumed to be greater and equal to zero.

The additional power needed to account for the losses across the transmission lines is supplied by production units in the system. This increases the total operating cost. Therefore in general, at least, one of these two state variables x_1 and/or x_2 can be greater than zero, when the LP algorithm reaches the optimal solution. Consequently, the linearized approximation of the losses in Eq. (4) can be expressed as in Eq. (6).

$$P_{Lij} \approx b + a\Delta\theta = -r_{ij}\frac{\Delta\theta_0^2}{x_{ij}^2} + 2r_{ij}\frac{\Delta\theta_0}{x_{ij}^2}(x_1 + x_2) \tag{6}$$

This approach provides the feedback from transmission losses to the optimal generation dispatch problem. The optimization problem can evaluate the trade-off between generation costs and transmission losses to find an optimum solution. Compared to the previous method where the power losses are subtracted equally from each side of the branch, in the linearized loss approximation shown here, the losses are subtracted from the side where it allows dispatching more low cost generations, such as wind power and minimize the total operating cost.

The calculated values of $\Delta\theta$ may deviate much from the assumed initial starting point $\Delta\theta_0$, and therefore there might be an error in the estimation of power loss. This can be observed in Fig. 5 as the difference between the green and red curves in the other points than $\Delta\theta_0$. For the small values of $\Delta\theta$ the power losses can even be negative, depending on the slope of the linearized power losses. This can be can be handled through an iterative process similar to the one described in iterative loss calculation, where the coefficients a and/or b in Eq. (4) are updated. Depending on the requirements for calculation speed, different approaches for upgrading the coefficients a and b can be adopted. The coefficient b is a part of the right hand side vector $\underline{\boldsymbol{B}}$, whereas a is a part of matrix $\underline{\boldsymbol{A}}$ in Eqs. (2).

3.2.1. Updating both coefficients "a" and "b" in linearized loss

Using the value of $\Delta\theta$ from previous step, a new linearized approximation of the transmission power losses can be estimated, as shown in Fig. 7. The new estimation of power losses (Step 2 shown in Fig. 7), for the given $\Delta\theta_1$, is closer to its "actual" value, as given by Eq. (3). The "feedback" of the transmission loss variation around the new operating point $\Delta\theta_1$ is also quite accurate compared to $\Delta\theta_0$. In this case, both vector $\underline{\boldsymbol{B}}$ and matrix $\underline{\boldsymbol{A}}$ in Eqs. (2) have been updated. For large scale power system models where many LP problems have to be solved successively, this can increase the computation burden significantly.

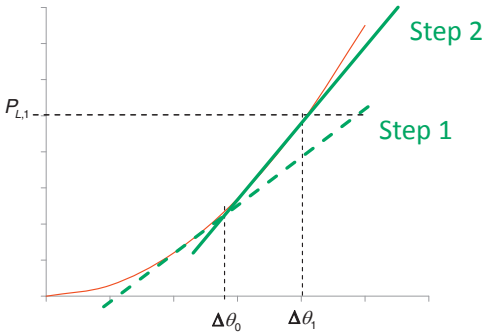

Fig. 7. Updating the linearized transmission loss approximation

3.2.2. Updating only coefficient a in the linearized loss case

In our simulation toolbox we benefit from the distinct advantage of allowing “warm starting” (*i.e.* using the previous solution as a start point for the next iteration). In this way, our LP problem shows a significant improvement in calculation time especially for cases where the DC optimal power flow has to be solved many times, typically running for every hour of a given year (8760 simulations). However, using a "warm starting" is possible as long as the left-hand sides of Eqs. (2) do not need to be updated at each iteration. Basically "warm starting" does not rely on updating matrix $\underline{\boldsymbol{A}}$ in Eqs. (2) for the entire simulation. Thus, using the "warm starting" possibility, we cannot update coefficient *a* in linearized approximation of transmission losses in Eq. (4).

Fig. 8 depicts the updated linearized approximation of transmission losses where only coefficient *b* has been updated with a new value. In this way, the power losses are accounted for in the optimization and there will also be a feedback of power loss variations to the optimization process. This feedback is now not as accurate as compared to the method updating both *a* and *b* coefficients, as previously described.

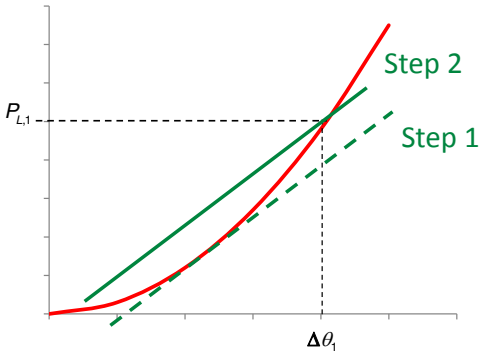

Fig. 8. Updating the linearized transmission loss approximation with fixed slope

4. Power system simulation tool (PSST)

The flow-based market model Power System Simulation Tool (PSST), developed by SINTEF Energy Research is selected as a simulation tool to study the effect of losses on large scale power systems [13]. PSST is a tool typically used for studying the effect of large scale penetration of Wind and PV power and the corresponding grid constrains and needed grid expansion. The main focus of PSST analysis has been to investigate possibilities for enhanced cross border energy exchange across the European power system to facilitate large scale Wind and PV power penetration [14, 15]. It is a flow-based market model that includes linear DC power flow in the optimization routine and accounts for wind variations, hydrological situations and network bottlenecks on production dispatch, demand and prices.

The PSST model is based on a perfect market assumption minimizing the total generation costs in the system for each hour of the simulation period. PSST finds the optimal annual generation dispatch with hourly resolution taking into account a detailed grid description. The high voltage network topology, generation and transfer capacities, wind power production and hydro power characteristics, as well as fuel price scenarios are incorporated in the model. Based on a DC optimal power flow the model minimizes the total generation costs on an hourly basis throughout the year.

The basic PSST simulation structure is displayed in Fig. 9. The inputs to PSST are split into constant and time dependent parameters. The electrical grid, generator capacities, respective marginal generator costs and the reservoir volume of hydro generators define constant for the whole simulation period. Wind and PV power production and load time series, water inflow into hydro reservoirs, reservoir levels and the subsequent water values [16] are updated for each simulation step. For more detail please see [17].

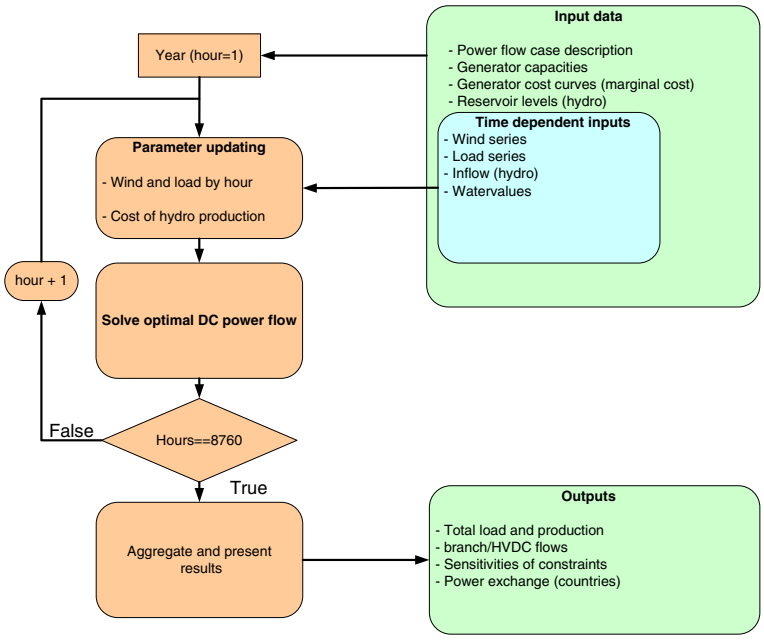

Fig. 9. The main simulation structure in PSST

5. Case studies

In order to perform a comparison study among different methodologies to apply active power losses in DC-OPF, we have tested aforementioned methodologies on the small scale case study and capture the effect of active power losses in the production dispatch and system operating cost.

5.1. Modified IEEE 9-bus case study

The study has been conducted on a modified IEEE 9-bus case portrayed in Fig. 10 [18]. As shown, the system is composed of three generators and three loads. The installed generation capacity is 50 MW more than the total demand which is assumed to cover the transmission power losses. Two main generators are installed at buses 1 and 3. The marginal cost of the generator installed at bus 1 is twice as high as the marginal cost for the one installed at bus 3.

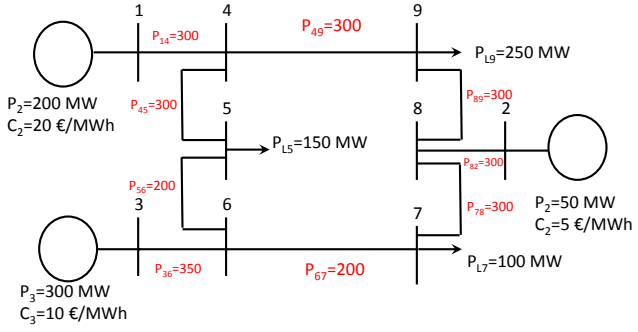

Fig. 10. Modified IEEE 9-bus system

AC-OPF is selected as a reference approach to assess the ***DC-OPF iterative*** (DC-OPF-I) approach, explained in *Section 3.1*, and ***DC-OPF linearized loss*** (DC-OPF-LL) with updating both coefficients, explained in Section *3.2.1*. The approaches are tested separately in different demand scenarios. We have increased the load from 20% to 100% and investigated the effect of loss on the operating cost, as shown in Fig. 11. The general trend is that the operating cost obtained with the DC-OPF-LL approach are lying somewhere between the AC-OPF and the DC-OPF-I approach.

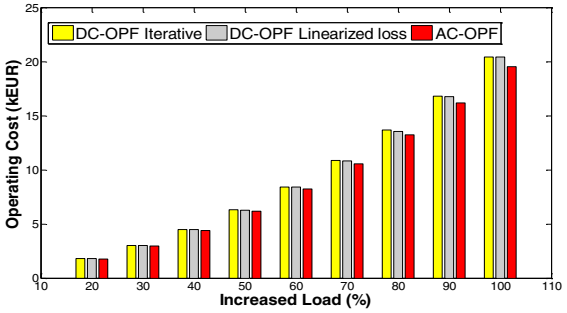

Fig. 11. Operating cost comparison in different approaches

Table 1 comprises the cumulative operating cost obtained in the all demand scenarios. As indicated in terms of operating cost, the linearized loss (DC-OPF-LL) method produces lower total costs than the iterative (DC-OPF-I) approach due to the feedback provide in the DC-OPF-LL method from active power losses to the production scheduling problem.

Table 1. Cumulative operating costs

Approaches	Operating costs (kEUR)
AC-OPF	83.05
DC-OPF-LL	85.46
DC-OPF-I	85.77

In order to study the impact of transmission active power losses, we compare the average generation utilization under different load scenarios obtained from the above approaches. As shown, DC-OPF-LL utilizes more the cheaper generator (G1 in this example) whereas the expensive generator (G3) is exploited more by DC-OPF-I approach, hence causing the operating cost to be greater in the DC-OPF-I than in the DC-OPF-LL approach.

Table 2. Average generation under different approaches to calculate active power losses in transmission system

Approaches	Average Generation (MWh)		
	G1(20 EUR/kWh)	G2(5 EUR/kWh)	G3(10 EUR/kWh)
AC-OPF	107.8	50	147.06
DC-OPF-LL	107	50	152.67
DC-OPF-I	109.89	50	150.58

Fig. 12 compares the computed active power losses in the above mentioned approaches with the reference approach AC-OPF (green curve). The gap between AC-OPF and DC-OPF-I (blue curve) can be reduced by using DC-OPF-LL approach (red curve). The cumulative absolute error in DC-OPF-I is calculated to be 17.31 MW (of 50MW margin) for all load scenarios whereas the error can be reduced significantly to 7.41 MW (of 50MW margin)

in DC-OPF-LL. Therefore, this is a strong indication towards the use of the linearized loss approach instead of iterative approach.

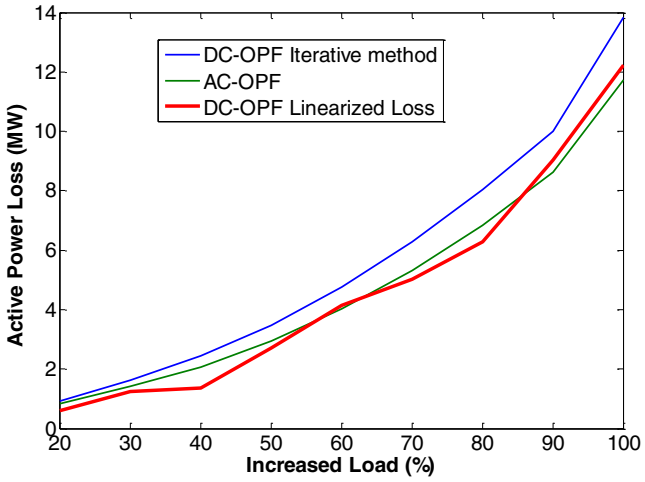

Fig. 12. Comparison of computed active losses in DC-OPF-I and DC-OPF-LL with reference approach AC-OPF along demand scenarios

However, as already described, for large systems we would like to use "warm starting" possibilities. Thus, we investigate now the performance of the so-called "*linearized approximation of losses with constant slope*" (DC-OPF-LL-CS) as illustrated in Fig. 8.

Fig. 13 shows the comparison of estimated active losses in DC-OPF-I and DC-OPF-LL-CS together with the reference AC-OPF approach across increased demand scenarios. As shown in the lower boundary of the curve, *i.e.* values smaller than 30% of increased demand, the computed losses are overestimated by DC-OPF-LL-CS compared to DC-OPF-I. This is due to the fact that the lower part of the actual transmission loss curve is quite flat and the iterative process for updating coefficient b might fail since $\Delta\theta$ is very small. Thus, a heuristic procedure is then needed to overcome this problem. In this respect, the solution would be switching to DC-OPF-I for low loads, *i.e.* the values below 40% increased demand and applying DC-OPF-LL-CS for medium and high loads, *i.e.* values greater than 40% of increased demand.

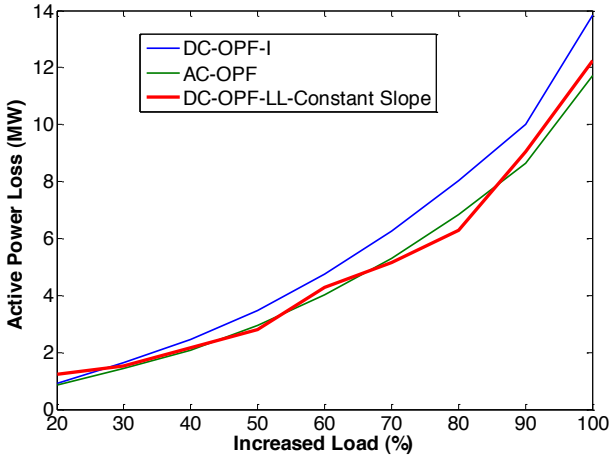

Fig. 13. Comparison of computed active losses in DC-OPF-I and DC-OPF-LL-CS with reference approach AC-OPF along demand scenarios

Fig. 14 is the result of applying the above mentioned heuristic (combined) approach. As shown, the estimated losses are decreased for low load scenarios. Using the combined approach may improve the calculation of transmission losses in a DC-OPF scheduling problem.

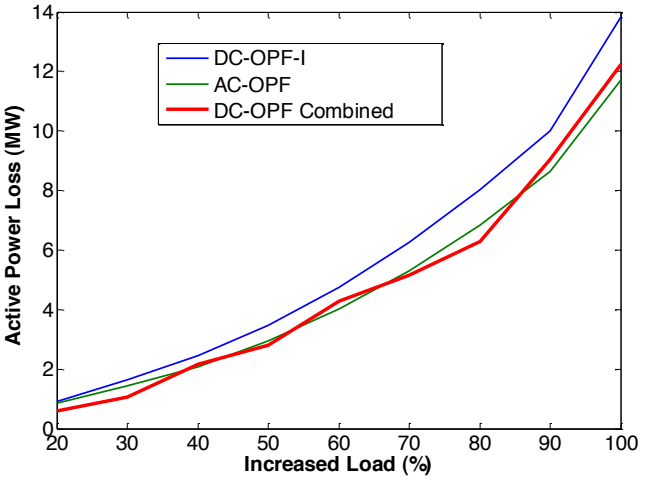

Fig. 14 Comparison of computed active losses in DC-OPF-I and combined approach with reference approach AC-OPF along demand scenarios

The results of accumulative system operating costs are presented in Table 3. Comparing the costs in different approaches reveals that the combined approach is lying between DC-OPF approach with updating all two coefficients (DC-OP-LL) and the method with constant slope (DC-OPF-LL-CS). On the other hand, "warm starting" functionality can be applied more accurately in the combined method.

Our overall conclusion based on the above analyses is that the best approach to apply transmission losses to large scale power system is the *combined approach*. This approach benefits from warm starting functionality which can improve the computational efficiency especially for the analysis where the scheduling problem should be solved for various operating situations for long time periods. Moreover, the results are quite accurate when comparing the iterative approach (DC-OPF-I) and the linearized loss with constant slope (DC-OPF-LL-CS).

Table 3. Comparison of different approached to calculate active power losses in the transmission system in terms of operating cost

Approaches	Operating costs (kEUR)
AC-OPF	83.05
DC-OPF-LL	85.46
DC-OPF-LL-Combined	85.56
DC-OPF-LL-CS	85.61
DC-OPF-I	85.77

5.2. Northern European case study

The next step is to investigate the performance of the approach on large scale power systems. As example, the Northern European power system including the Scandinavian countries and Germany is considered. PSST model dataset and scenarios are used for the analysis. The target year for this study is 2030 and the offshore wind parks are assumed to be built in the North Sea. The installed wind power capacity according to the estimations made by the European Wind Energy association (EWEA) accumulates up to 369 GW in 2030, out of which more than 95 GW

will be offshore wind power production installed in the North Sea [19, 20]. Fig. 15 schematically illustrates the case study for our analysis where three major offshore wind clusters in the North Sea are considered with installed capacities as mentioned in the Fig. 15. It is expected that NorGer HVDC cable interconnecting the German and Norwegian electricity systems is operational by 2030. The NorGer cable with a capacity of approximately 1400 MW is intended to deliver German wind power to Norway or Norwegian hydropower to Germany and generally supposed to help balancing fluctuations due to generation of electricity from RES. In this part, we consider how the inclusion of transmission active power losses can affect offshore wind power and NorGer interconnection utilization within a DC-OPF scheduling problem.

Fig. 15. The Northern European Continental system including

The scheduling problem using DC-OPF is ran for 8760 hours (one year) and the impact of transmission losses on utilization of offshore wind power production is investigated. Fig. 16 shows a short window (20 days) of the simulated total offshore wind power utilization in three offshore clusters marked in Fig. 15. Two approaches of applying transmission losses, *i.e.* iterative approach (DC-OPF-I blue curve) versus linearized approximation loss approach (DC-OPF-LL-CS red curve) are compared.

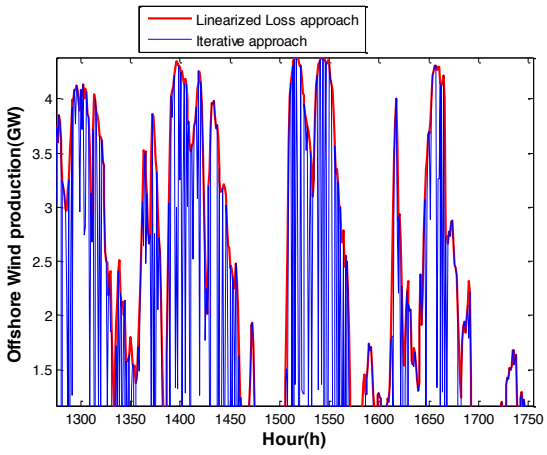

Fig. 16. Offshore wind utilization in the North Sea

As shown in Fig. 16, applying transmission losses using iterative approach (DC-OPF-I, blue curve) causes wind production curtailment. This is due to the fact that offshore wind power facilities are located far away from the load centers and the internal grid is more constrained by taking transmission losses into account. However, this effect does not appear in the linearized loss approach (DC-OPF-LL-CS, red curve) demonstrating the effectiveness of considering feedback from loss calculation to dispatch scheduling problem. The feedback in the DC-OPF-LL-CS method helps the scheduling problem to relieve the expected grid bottlenecks more 'optimally' allowing high penetration of offshore wind power to the production mix, therefore reducing the operating costs. Table 4 shows this effect in terms of annual operating cost for three cases. These cases include the dispatch problem without taking into account transmission losses as well as tacking losses into account using linearized approximation loss and iterative approach. The simulation results shown in the table indicate that: *i)* transmission losses increase the total operating costs; *ii)* use of the linearized approximation to losses translates into a 35% lower operational costs than the iterative method.

Table 4. Annual operating costs

Cases	Annual Operating costs (bn EUR)
No loss	41.43
Linearized loss	43.41
Iterative	44.46

The HVDC exchange values in PSST are handled by two controllable values between minimum and maximum cable capacity. The controllable values model the withdrawal of power from one end and the injection power at the other end of the cable. The difference between these two values models the transmission losses across the HVDC interconnection. The transmission losses in HVDC cable are considered as the constant percentage of the exchange power through the cable. The percentage of transmission loss in HVDC cable depends on the cable technology. In this work, we have used 3.5% for line commutated converter-LCC HVDC type and 5% for voltage source converter-VSC HVDC type. The NorGer HVDC cable is assumed to be LCC type and therefore the loss percentage is equal to 3.5% [2].

Duration curves for annual exchange of energy across NorGer interconnection are depicted in Fig. 17. The utilization of the interconnection is reduced significantly in the case with active power losses. These results show: *i)* firstly a redistribution of the wind power injection into the German mainland grid in order to cover land and grid losses; *ii)* secondly there is a period of time through the year with zero exchange (blue curve between red vertical lines) because the price difference at both ends of HVDC cable is not high enough to cover the losses across the cable and therefore no exchange power occurs at the HVDC interconnection.

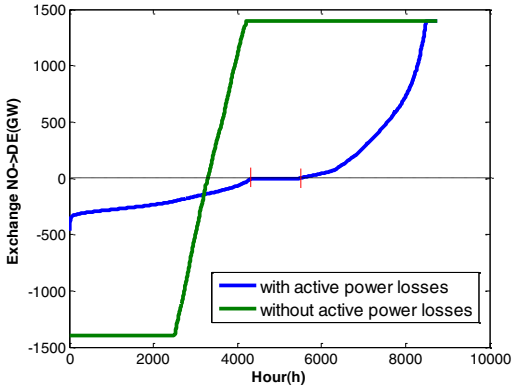

Fig. 17. Utilization of the NorGer interconnection (the positive values mean flow from Norway to Germany and negative values represent flow from Germany to Norway

Fig. 18 represents the price difference (showed by the blue curve) that cannot cover the transmission losses across the NorGer HVDC interconnectors, hence no power exchange between Germany and Norway. The red curves determine a dead-band for these price differences. In contrast to the lossless system when the small price differences can change the flow direction on HVDC interconnection from full import to full export, in system with transmission losses the price difference should be greater than dead-band defined in Fig. 18, so power exchange can occur on the HVDC cable. When the price difference is out of the dead-band, transmission losses can be "covered" on the interconnection and there can be an exchange power from low price system to high price system. The width of the dead-band can be determined based on the underlying analysis presented in [21], which can be calculated by use Eq. (7).

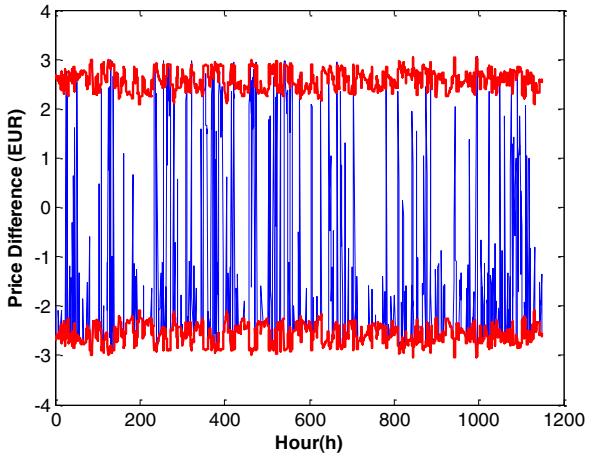

Fig. 18. Price difference at both ends of NorGer HVDC interconnection when there is no power exchange

According to Eq. (7), the dead-band width is the function of the lower price at both ends of the interconnection multiplied by the loss percentage of the interconnection which is equal to 3.5% in the case of NorGer HVDC cable.

$$\pi_{ij} = Min\left(P_i, P_j\right) \cdot \%P_{loss} \tag{7}$$

6. Conclusion

This paper presents a comparison analysis of two approaches to include transmission active losses in optimal generation scheduling problem using DC-OPF. These approaches are iterative approach (DC-OPF-I) and linear approximation of transmission losses around the operating point (DC-OPF-LL/-LL-CS). Including transmission active power losses can influence the generation scheduling, power exchanges between countries, and offshore wind power utilization and thereby affect the socio-economic costs significantly.

The proposed approaches are applied to modified IEEE 9-bus test system. The results demonstrate that linearized approximation of losses provides a more optimal way to take into account transmission losses in DC-OPF generation scheduling problems. The linearized approximation of losses provides feedback from transmission loss calculations to the generation scheduling problem, thus the optimization algorithm can evaluate the trade-off between generation cost and transmission losses to find an optimum solution to cover losses. The linearized approximation approach requires iterations to update the estimation of power losses meaning that both coefficients of the linearized approximation are updated corresponding to the new power system operating point. In order to solve DC-OPF problems with large scale power systems using the PSST tool and within reasonable calculation time, the so-called "warm starting" functionality is desired. However, using "warm starting" functionality prevents updating the slope of the linearized approximation of the transmission losses. The results of the different methods investigated on the IEEE 9-bus test system demonstrate that the best alternative is to use the combined method where the iterative approach can be used for low load scenarios and linearized method for medium and high load scenarios.

A preliminary test on the Northern European shows the importance of integrating transmission loss calculation in the generation scheduling problem. This is a case especially for offshore wind facilities typically located far away from load centers. For these cases, DC OPF generation scheduling problem aims to optimize the reduction of internal grid bottlenecks and the dispatching of units with lowest possible operational production costs. Moreover, transmission losses can reduce the value of power exchange across HVDC interconnections between countries, since the price differences should be sufficient to cover the losses along the interconnections. A dead-band based on the price differences at both ends of the HVDC interconnections and HVDC loss percentage is defined determining the required minimum price difference needed in order to allow exchange power along the HVDC interconnections.

Acknowledgements

This work is financially supported by NOWITECH FME centre (www.nowitech.no).

References

[1] Veum K, Cameron L, Huertas Hernando D, Korpås M, Roadmap to the deployment of offshore wind energy in the Central and Southern North Sea (2020 - 2030), IEE-EU Wind Speed Project, Final Report; 2011, [online]. Available: http://www.windspeed.eu/.

[2] Farahmand H, Huertas-Hernando D, Warland L, Korpås M, Svendsen HG, Impact of system power losses on the value of an offshore grid for North Sea offshore wind, 2011 IEEE Trondheim PowerTech Conference; 19-23 June 2011.

[3] Helseth A, A linear optimal power flow model considering nodal distribution of losses, 9th International Conference on the European Energy Market (EEM2012); 10-12 May 2012.

[4] Stott B, Jardim J, Alsac O, DC Power Flow Revisited, IEEE Transactions on Power Systems 2009; 24:3; p. 1290-1300.

[5] Wood AJ, Wollenberg BF, Power Generation & Control. 2nd ed. USA: Wiely-Interscience; 1996.

[6] Farahmand H, Hosseini SMA, Doorman GL, Fosso OB, Flow based activation of reserves in the Nordic power system, IEEE Power and Energy Society General Meeting Conference; 25-29 July 2010.

[7] Fangxing L, Rui B, DCOPF-Based LMP Simulation: Algorithm, Comparison With ACOPF, and Sensitivity, IEEE Transactions on Power Systems 2007; 22:4; p. 1475-1485.

[8] Litvinov E, Tongxin Z, Rosenwald G, Shamsollahi P, Marginal loss modeling in LMP calculation, IEEE Transactions on Power Systems 2004; 19:2; p. 880-888.

[9] Sarkar V, Khaparde SA, DCOPF-Based Marginal Loss Pricing With Enhanced Power Flow Accuracy by Using Matrix Loss Distribution, IEEE Transactions on Power Systems 2009; 24:3; p. 1435-1445.

[10] Zechun H, Haozhong C, Zheng Y, Furong L, An Iterative LMP Calculation Method Considering Loss Distributions, IEEE Transactions on Power Systems 2010; 25:3; p.1469-1477.

[11] Hobbs BF, Drayton G, Fisher EB, Lise W, Improved Transmission Representations in Oligopolistic Market Models: Quadratic Losses, Phase Shifters, and DC Lines, IEEE Transactions on Power Systems 2008; 23: 3; p. 1018-1029.

[12] Norbiato dos Santos T, Diniz AL, A Dynamic Piecewise Linear Model for DC Transmission Losses in Optimal Scheduling Problems, IEEE Transactions on Power Systems 2011; 26:2; p. 508-519

[13] Korpås M, Warland L, Tande JO, Uhlen K, et al., Further developing Europe's power market for large scale integration of wind power - grid modelling and power system data, IEE-EU TradeWind project, Final report; 2008, [online]. Available: http://www.uwig.org/TradeWind.pdf.

[14] Farahmand H, Jaehnert S, Aigner T, Huertas-Hernando D, Possibilities of Nordic hydro power generation flexibility and transmission capacity expansion to support the integration of Northern European wind power production: 2020 and 2030 case studies, Deliverable D16.3 EUFP7 TWENTIES project, SINTEF Energy Research; 2013, [online]. Available: http://www.twenties-project.eu/system/files/D16.3_FINAL2013.pdf.

[15] Svendsen HG, Warland L, Korpås M, Huertas-Hernando D, Report describing the power market model, data requirements and results from analysis of initial grid designs, Deliverable 6.1 IEE EU OffshoreGrid project, Sintef Energy Research; 2010, [online]. Available: http://www.offshoregrid.eu/images/pdf/offshoregrid_d6.1%20power%20market%20modelling.pdf.

[16] Wolfgang O, Haugstad A, Mo B, Gjelsvik A, Wangensteen I, Doorman G, Hydro reservoir handling in Norway before and after deregulation, Energy 2009; 34: 10; p. 1642-1651.

[17] Farahmand H, Integrated Power System Balancing in Northern Europe - Models and Case Studies, Department of Electrical Power Engineering, Norwegian University of Science and Technology; 2012.

[18] Zimmerman RD, Murillo-Sánchez CD, Gan D, A MATLAB Power System Simulation Package, Available: http://www.pserc.cornell.edu//matpower/.

[19] Cutululis NA, Litong-Palima M, Zeni L, Gøttig A, Detlefsen N, Sørensen P, Offshore Wind Power Data, Deliverable D16.1 EUFP7 TWENTIES project , DTU Wind Energy; 2012, [online]. Available: http://www.twenties-project.eu/node/18.

[20] Zervos A, Kjaer C, Pure wind: wind energy scenarios up to 2030, Technical Report, European Wind Energy Association (EWEA); 2008, [online]. Available: http:\\www.ewea.org.

[21] Jaehnert S, Wolfgang O, Farahmand H, Völler S, Huertas-Hernando D, Transmission expansion planning in Northern Europe in 2030-Methodology and analyses, Energy Policy 2013; 61; p. 125-139.